LBL-13365

Lawrence Berkeley Laboratory
UNIVERSITY OF CALIFORNIA

Materials & Molecular
Research Division

Presented at the 29th Midwest Solid State Conference, Argonne National Laboratory, Chicago, IL, September 24-26, 1981; and to be published in Novel Materials and Techniques in Condensed Matter, Elsevier North Holland, New York

NONLINEAR OPTICAL TECHNIQUES FOR SURFACE STUDIES

Y.R. Shen

September 1981

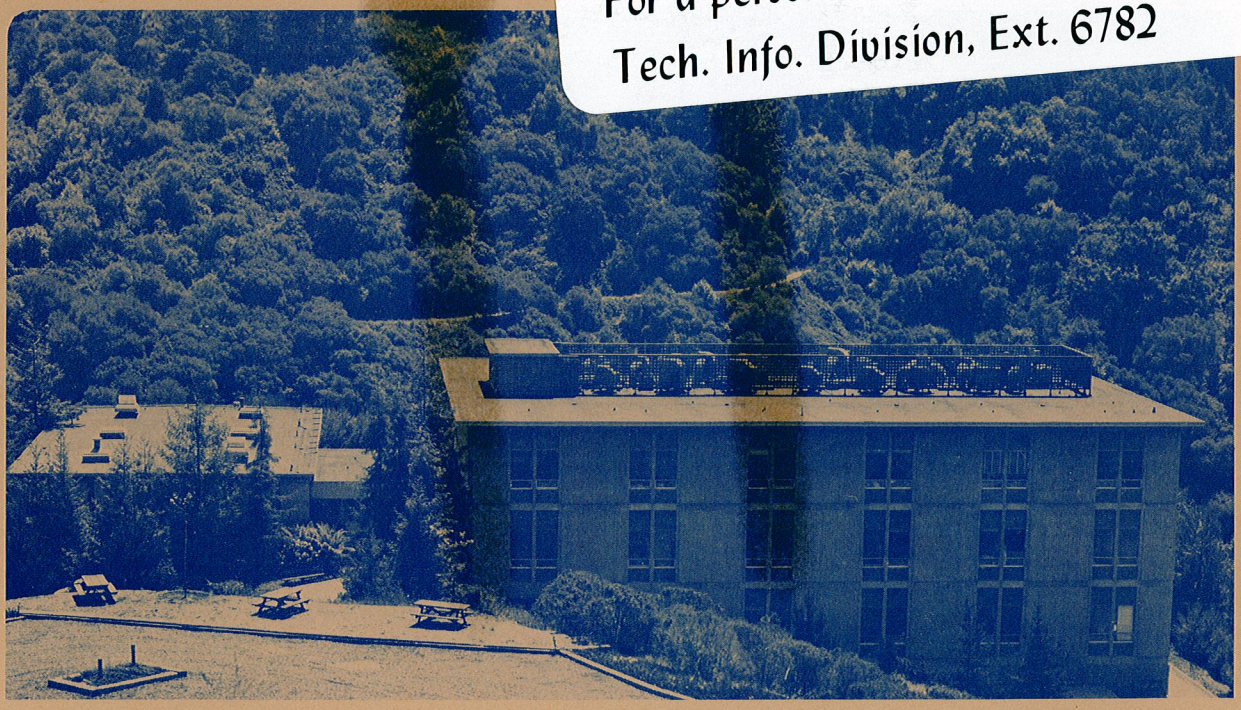

Prepared for the U.S. Department of Energy under Contract W-7405-ENG-48

NONLINEAR OPTICAL TECHNIQUES FOR SURFACE STUDIES

Y. R. SHEN
Department of Physics, University of California, and Materials and Molecular Research Division, Lawrence Berkeley Laboratory, Berkeley, California 94720

ABSTRACT

Recent effort in developing nonlinear optical techniques for surface studies is reviewed. Emphasis is on monolayer detection of adsorbed molecules on surfaces. It is shown that surface coherent antiStokes Raman scattering (CARS) with picosecond pulses has the sensitivity of detecting submonolayer of molecules. On the other hand, second harmonic or sum-frequency generation is also sensitive enough to detect molecular monolayers. Surface-enhanced nonlinear optical effects on some rough metal surfaces have been observed. This facilitates the detection of molecular monolayers on such surfaces, and makes the study of molecular adsorption at a liquid-metal interface feasible. Advantages and disadvantages of the nonlinear optical techniques for surface studies are discussed.

INTRODUCTION

In surface science research, the physics and chemistry of adsorbed molecules on surfaces are often considered to be most important. Detection of molecular monolayers or submonolayers is essential for such studies. Various techniques have already been developed for this purpose; yet only a few can be used to probe the microscopic properties of adsorbed molecules [1]. Among them, the photoemission spectroscopy is useful for studying the electronic transitions of the molecules in the far uv and X-ray region, while the electron loss spectroscopy is capable of probing the vibrational transitions, but the spectral resolution is limited. Inelastic electronic tunneling spectroscopy [2], on the other hand, can yield high resolution vibrational spectra, but the molecules must be incorporated into a metal-insulator-metal junction and studied at low temperature. Conventional optical techniques can also be used for surface studies with possible high spectral resolution [1]. They, however, have their own difficulties. The well-known ellipsometry technique can detect molecular monolayers, but it lacks the spectral selectivity. Infrared spectroscopy is generally not sensitive enough to detect monolayers on smooth surfaces except perhaps in a narrow spectral region [3]. Recent advance in this area using a low-temperature thermal detection scheme allows the monolayer detection [4], but the technique is limited to surface studies at liquid He temperature. Spontaneous Raman spectroscopy, in principle, is capable of detecting monolayers, but the Raman signal is usually masked by the luminescence background. New spectroscopic techniques which are both sensitive and of high resolution over a broad spectral region are clearly needed.

Recently, with the advent of tunable lasers, nonlinear optical spectroscopic techniques have been developed quite rapidly. They are often characterized by high sensitivity and fine spectral resolution. It is then natural to ask whether these techniques can be used for surface studies. Indeed, there has been some success in this respect in the past few years. We have found that surface coherent antiStokes Raman spectroscopy (CARS) with picosecond pulses can have the sensitivity of detecting submonolayers of adsorbed molecules [5].

Heritage [6] and Levine et al. [7] have demonstrated that picosecond Raman gain spectroscopy can be used to obtain Raman spectra of thin films and molecular monolayers. The recent discovery of surface enhanced Raman scattering (which being a two-photon transition can also be considered as a nonlinear optical process) has led to the possibility of studying adsorbed molecules on some rough metal surfaces by Raman spectroscopy [8]. We then realize that such surface enhancement should also happen to other nonlinear optical processes [9]. Study of adsorbed molecules on those rough metal surfaces by surface nonlinear optics then also becomes feasible [10]. In fact, a simple estimate would show that even a monolayer of adsorbed molecules on smooth surfaces can yield a detectable second-harmonic or sum-frequency signal. This suggests the possibility of studying adsorbed molecules by sum-frequency spectroscopy.

In this paper, we shall review the various nonlinear optical techniques for surface studies, with emphasis on our own recent work on surface CARS and detection of adsorbed molecules by second harmonic generation through surface enhancement. To begin with, we give a brief introduction on surface nonlinear optics [11]. It is then followed by discussion on surface CARS, surface-enhanced nonlinear optical effects, and detection of adsorbed molecules by second harmonic generation. The advantages and disadvantages of the nonlinear optical techniques over the conventional techniques for surface studies will be pointed out.

SURFACE NONLINEAR OPTICS

Surface nonlinear optics deals with nonlinear optical effects at an interface. Depending on the processes, it is to some degree affected by the material properties at the interface, and may therefore be used to study the interface. Yet, the subject has not received much attention since the early investigations of Bloembergen and coworkers on second-harmonic reflection from a surface [12]. As in the bulk case, surface nonlinear optical effects are governed by the nonlinear polarization $\vec{P}^{NL}$ induced around the interface by the incoming pump fields. Being a collection of oscillating dipoles, the nonlinear polarization acts as a source of radiation to generate the nonlinear output. We will consider only surface nonlinear wave mixing here. The formal derivation follows the usual solution of the wave equation with $\vec{P}^{NL}$ as a driving source [11].

$$[\nabla \times (\nabla \times) - \omega^2\varepsilon/c^2]\vec{E}(\omega) = (4\pi\omega^2/c^2)\vec{P}^{NL}(\omega) \tag{1}$$

with $\nabla \cdot (\varepsilon\vec{E} + 4\pi\vec{P}^{NL}) = 0$ where, for example, $\vec{P}^{NL}(2\omega) = \overleftrightarrow{\chi}^{(2)}:\vec{E}(\omega)\vec{E}(\omega)$ for second harmonic generation, $\vec{P}^{NL}(\omega = 2\omega_1 - \omega_2) = \overleftrightarrow{\chi}^{(3)}:\vec{E}_1(\omega_1)\vec{E}_1(\omega_1)\vec{E}_2^*(\omega_1)$ for CARS. Note that $\vec{P}^{NL} \propto \exp(i\vec{k}_s \cdot \vec{r})$ with $\vec{k}_s = 2\vec{k}_1(\omega)$ for second harmonic generation, and $\vec{k}_s = 2\vec{k}_1(\omega_1) - \vec{k}_2(\omega_2)$ for CARS. The solution of Eq. (1) with appropriate boundary conditions is fairly straightforward, but tedious [11, 12]. Its essential features can, however, be spelled out directly from physical argument. (1) The output field amplitude must have the form

$$|E_{out}| = |\gamma_{1,\parallel}P^{NL}_{1,\parallel} + \gamma_{1,\perp}P^{NL}_{1,\perp} + \gamma_{2,\parallel}P^{NL}_{2,\parallel} + \gamma_{2,\perp}P^{NL}_{2,\perp}| \tag{2}$$

where the subindices 1 and 2 refer to the two boundary media at the interface, and $\parallel$ and $\perp$ refer to the components parallel and perpendicular to the interface. The γ's are constants governing the efficiency of the induced dipole radiation. (2) If $\vec{P}^{NL}$'s are confined to layers of thickness much less than a wavelength, then γ_i is proportional to the layer thickness d_i. (3) The output power in the medium with a dielectric constant ε is given by

$$\mathcal{P}(\omega) = (c\varepsilon^{1/2}/2\pi)\int |E_{out}(\omega)|^2 dA \tag{3}$$

where the integration is over the nonlinearly excited surface. (4) From a flat smooth interface, the coherent output is highly directional, with its direction determined by the wavevector component $k_{s\|}$ of $\vec{P}^{NL}$, since by boundary condition, the output wavevector should have its component along the interface equal to $k_{s\|}$.

It is seen from Eqs. (2) and (3) that for large nonlinear output, both γ and $\vec{P}^{NL}$ must be large. For a large $\vec{P}^{NL}$, the nonlinear susceptibility $\overleftrightarrow{\chi}^{(n)}$ and the pump fields should be large. The former depends on the material and can be greatly enhanced near resonance. The latter are often limited by optical damage, but can be enhanced using surface wave excitation.

SURFACE COHERENT ANTISTOKES RAMAN SCATTERING

One of the potentially useful nonlinear spectroscopic methods for studies of thin films and adsorbed molecules is CARS [5]. The corresponding nonlinear susceptibility of the probed medium is

$$\chi^{(3)}(\omega = 2\omega_1 - \omega_2) = \chi^{(3)}_{NR} + \chi^{(3)}_R \tag{4}$$

$$\chi^{(3)}_R = \frac{A}{[(\omega_1 - \omega_2) - \omega_v] + i\Gamma}$$

which shows the resonant enhancement as $(\omega_1 - \omega_2)$ approaches the vibrational frequency ω_v. The antiStokes output, being proportional to $|\chi^{(3)}|^2$, can therefore be used to probe the Raman resonance. For the 992 cm^{-1} mode of benzene, for example, $\chi^{(3)}_{NR} \simeq 4 \times 10^{-14}$ esu and $(\chi^{(3)}_R)_{max} \simeq 3 \times 10^{-13}$ esu [13]. With $(\chi^{(3)}_R)_{max}$ of this magnitude, the CARS signal can be easily detected in bulk benzene with pulsed laser intensity of the order of 1 MW/cm^2. In the case of a thin film of benzene, however, the signal would be hardly detectable even if pulsed lasers with near-breakdown intensity are used. Then, in order to enhance the surface CARS signal, we must increase the pump field $E_i(\omega_i)$ without increasing the incoming laser intensity. This can be done by using surface plasmons as pump fields.

Surface plasmons are surface electromagnetic waves confined to the region around an interface between a metal and a dielectric, and propagating along the interface [14]. In the simple case of a plane interface ($z = 0$) with metal on one side ($z < 0$) and dielectric on the other side ($z > 0$), the surface plasmon appears to be transverse magnetic and has the form

$$\vec{E} = \vec{\mathcal{E}}_D e^{iK_{\|}\rho - \alpha_D z} \quad \text{for } z > 0$$

$$= \vec{\mathcal{E}}_M e^{iK_{\|}\rho - \alpha_M z} \quad \text{for } z < 0 \tag{5}$$

where

$$K_{\|} = K'_{\|} + iK''_{\|} = \frac{\omega}{c}\left(\frac{\varepsilon_D \varepsilon_M}{\varepsilon_D + \varepsilon_M}\right)^{1/2}$$

$$\alpha_D = [K^2_{\|} - (\omega^2 \varepsilon_D / c^2)]^{1/2} = 2\pi\varepsilon_D/\lambda\,|\varepsilon_D + \varepsilon_M|^{1/2}$$

$$\alpha_M = [K^2_{\|} - (\omega^2 \varepsilon_M / c^2)]^{1/2} = 2\pi|\varepsilon_M|/\lambda\,|\varepsilon_D + \varepsilon_M|^{1/2}.$$

ε_M and ε_D are the dielectric constants of the metal and dielectric respectively, with $\varepsilon_M < 0$, $\varepsilon_D > 0$, and $|\varepsilon_M| > \varepsilon_D$. It is seen from Eq. (5) that the surface plasmon field is confined to a layer of less than a wavelength. Then, if by some means, an input laser beam can be coupled with nearly 100% efficiency into a surface plasmon wave, then the field intensity at the surface is greatly enhanced, making the surface nonlinear optical effects more easily observable [15].

There are a number of methods one can use to excite a surface plasmon [11]. One of them commonly used is the Kretschmann method shown in Fig. 1(a) [16].

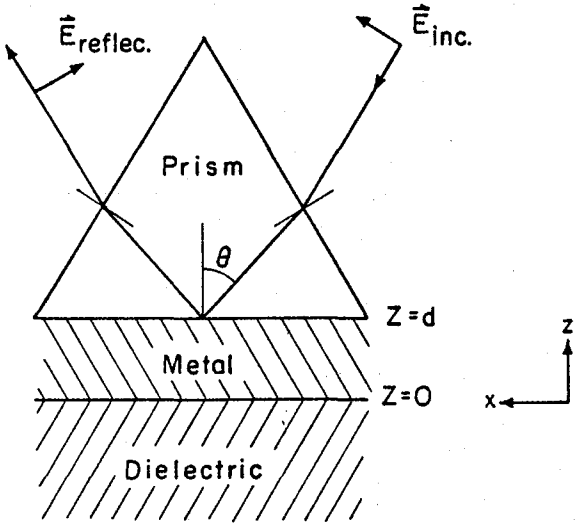

Fig. 1(a). Kretschmann geometry for exciting surface plasmons.

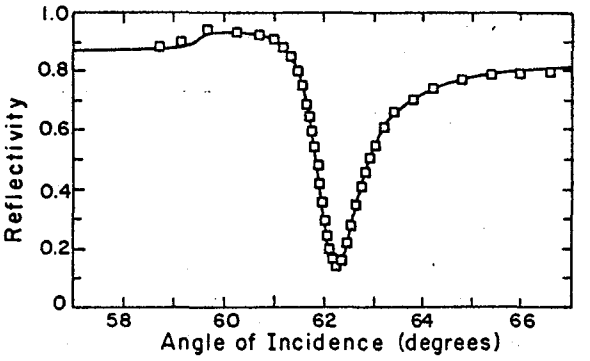

Fig. 1(b) Reflectivity versus the angle of incidence θ showing the sharp dip resulting from surface plasmon excitation. The solid curve is a theoretical curve that fits the experimental data points.

The surface plasmon at the metal-dielectric interface is excited when the incoming beam in the glass prism has a wavevector component along the interface equal to $K_{\|}'$. Experimentally, this is seen by a sharp reflectivity drop at the proper angle of incidence, indicating that most of the incoming beam power is coupled into the surface plasmon. An example is shown in Fig. 1(b). For a metal-air interface with ~ 100% coupling efficiency, the field amplitude at the interface can be enhanced by a factor of 20 through surface plasmon excitation. For a metal-dielectric interface with $\varepsilon_D \simeq 2.5$, the enhancement can be ~ 10. Therefore, if surface plasmons are used as pump fields in surface CARS, the nonlinear polarization $\vec{P}^{NL}$ at the metal-dielectric interface can be enhanced by a factor of $\sim 10^3$, and the resulting CARS signal by $\sim 10^6$. Even with a less ideal metal-dielectric interface so that the field enhancement is only 5, the surface CARS signal will be enhanced by $\sim 1.5 \times 10^4$. The signal is further enhanced if the antiStokes generation is phase matched, i.e., the generated antiStokes wave is also a surface plasmon with $\vec{k}_{s,\|} = 2\vec{k}_{1,\|} - \vec{k}_{2,\|} = \vec{K}_{\|}'(\omega = 2\omega_1 - \omega_2)$. This is formally described by a factor $(k_{s,\|} - K_{\|})$ in the denominator of the γ's in Eq. (2) [17].

The feasibility of doing CARS with surface plasmons has actually been demonstrated using the setup in Fig. 2 [5]. The surface plasmons at ω_1(6943 Å) and ω_2 (7456 Å) are excited through the glass prism. The relative angle between $\vec{k}_{1,\|}$ and $\vec{k}_{2,\|}$ is adjusted so that the phase matching condition for antiStokes surface plasmon generation is satisfied. The spectrum of $|\chi^{(3)}(\omega = 2\omega_1 - \omega_2)|^2$ is then obtained by scanning $(\omega_1 - \omega_2)$ and should show a resonant peak at $\omega_1 - \omega_2 \simeq \omega_v$. An example is shown in Fig. 3, where benzene is the dielectric medium being studied. The experimental data are well described by the curve of $|\chi^{(3)}|^2$ with $\chi^{(3)}$ given in Eq. (4). A detailed calculation also predicts an antiStokes power output

$$\mathcal{P}(\omega) = 1.1 \times 10^{-34} \mathcal{P}_1^2 \mathcal{P}_2 / \phi^4 \quad \text{ergs/sec.} \tag{6}$$

where $\mathcal{P}_1$ and $\mathcal{P}_2$ are the incoming pump power in ergs/sec. and ϕ is the pump beam waist at the interface. For input pulses with pulsewidth T = 25 nsec, ϕ =

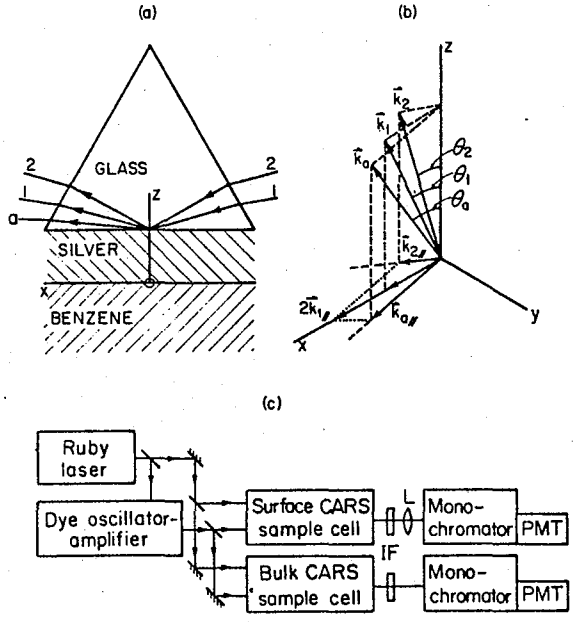

Fig. 2. (a) Prism-metal-liquid assembly for surface CARS measurement. Beam 1 is in the x-z plane, but beam 2 and the output are not. (b) Wavevectors in the glass prism with components in the x-y plane phase-matched. (c) Diagram of the apparatus: IF is an interference filter and L is a lens

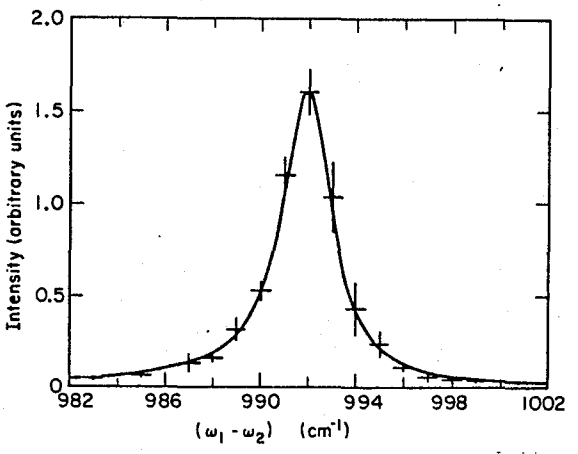

Fig. 3. AntiStokes signal vs $\omega_1 - \omega_2$ near resonance.

0.5 cm^2, and pulse energies $\mathcal{P}_1 T$ = 0.5 mJ and $\mathcal{P}_2 T$ = 5 mJ, the expected anti-Stokes output is $\mathcal{P}T = 2.5 \times 10^5$ photons/pulse, which agrees very well with the observed signal of 2×10^5 photons/pulse. The antiStokes output is a highly directional coherent beam coupled out through the prism in the direction determined by $k_{\parallel} = K'_{\parallel}$. Other characteristic features of the coherent antiStokes output are also in agreement with theory. It is interesting to note that the effective interaction length here is limited by the attenuation length of surface plasmons, which is very short, of the order of 10 μm on silver, because of the large attenuation constant in metal. Therefore, the CARS signal will not be significantly changed even if the dielectric medium is absorbing as long as the absorption is not too strong. This has actually been experimentally verified [18].

We realize that because of the short penetration length of surface plasmons into the dielectric, only a dielectric layer of $\lesssim$ 1000 Å effectively contributes to the CARS signal in the above case. Yet the signal is still easily detectable. This suggests that the scheme should be useful to study thin films and overlayers, and possibly surface-specific problems. If the signal can be increased by another few orders of magnitude, then even the spectroscopic study of adsorbed molecular monolayers should be possible.

To increase the CARS signal, we must increase the pump field intensities, but the latter are often limited by optical damage on the metal surface. Fortunately, in many cases, the optical damage threshold is set by energy/cm^2 per pulse impinged on the surface. Assuming that this is true for pulses with pulsewidths less than 100 nsec., we can then increase the pump field intensities by simply reducing the pulsewidth. According to Eq. (6), if we take a reasonable damage threshold to be 20 mJ/cm^2, then with 10-psec pump pulses of energy 10 μJ/pulse focused to a beam waist of 10 μm at the interface, the expect-

ed signal is $\sim 10^{11}$ photons/pulse from benzene. We should remember that the signal here mainly comes from a ~ 1000 Å layer (~ 100 monolayers) of benzene at the interface. Since the coherent signal is proportional to the square of the number of radiating molecules, we reach the conclusion that even a single monolayer of benzene molecules can yield a CARS output of $\sim 10^7$ photons/pulse. Therefore, surface CARS studies of adsorbed molecular monolayers certainly appears feasible.

SURFACE RAMAN GAIN SPECTROSCOPY

Among other coherent Raman spectroscopic techniques, stimulated Raman gain spectroscopy has attracted much attention because of its high sensitivity, its ability to suppress luminescence, and its resulting spectrum free of nonresonant background [19]. From the simple theory of stimulated Raman scattering, the Stokes output field can be written as

$$\begin{aligned} E_s &= E_{so} e^G \\ &\simeq E_{so}(1 + G) \quad \text{if } G \ll 1 \end{aligned} \tag{7}$$

where

$$G \propto [\mathrm{Im}\chi_R^{(3)}(\omega_s = \omega_s + \omega_\ell - \omega_\ell)]E_\ell E_\ell^*.$$

We can actually consider the case for $G \ll 1$ also as a wave mixing process with an output

$$\begin{aligned} \Delta E_s &= E_{so} G \\ &\propto [\mathrm{Im}\chi_R^{(3)}]E_{so}E_\ell E_\ell^*. \end{aligned}$$

The Raman gain is proportional to the pump intensity $|E_\ell|^2$. Therefore, if the pump energy impinging on the medium should be limited, the use of picosecond pulses can greatly increase the sensitivity of the Raman gain spectroscopy. With continuously mode-locked lasers and synchronous detection scheme, nearly shot noise limited performance can be achieved. Detection of a gain as small as $G \sim 10^{-8}$ is possible [20]. The technique should then be sensitive enough to record the Raman spectrum of a molecular monolayer. Indeed, Heritage [6] has succeeded in observing the Raman spectrum of a monolayer of p-nitrobenzoic acid on aluminum oxide, and Levine and coworkers [7] has obtained the Raman spectrum of a 20 Å layer of silicon.

Since the gain is proportional to the pump intensity, it can certainly be further enhanced by using surface plasmons as the pump field. An enhancement of one to two orders can be expected.

SURFACE SECOND-HARMONIC AND SUM-FREQUENCY GENERATION

While third-order nonlinear processes can be used to detect molecular monolayers, one may expect that second-order processes can also do the job. This is actually very interesting because in a medium with inversion symmetry, the second-order nonlinear susceptibility of the bulk vanishes in the electric dipole approximation. The surface atomic or molecular layer has, however, no inversion symmetry. Its contribution to $\chi^{(2)}$ is therefore equivalent to the electric quadrupole and magnetic dipole contribution to $\chi^{(2)}$ from about 1000 layers of atoms or molecules in the bulk [12]. In actual experiments, the effective interaction length is given by the inverse of the wavevector mismatch $|\Delta k|$. Then, if $|\Delta k| \gg 10^4$ cm^{-1}, the surface contribution to $\chi^{(2)}$ may dominate over

the bulk contribution. Thus, the second-order processes may allow us to look selectively at the interface.

The second-order process is in fact sensitive enough to detect a surface monolayer by shining the pump beams directly on the surface. This can be seen from the following estimate. The detailed calculation of second harmonic generation from a molecular monolayer predicts a signal [12]

$$S \simeq \frac{256\pi^3\omega}{\hbar c^3} |N_A\alpha^{(2)}|^2 (\mathcal{P}_1 T/A)^2 (A/T) \text{ photons/pulse} \qquad (8)$$

where N_A is the surface density of molecules in cm^{-2}, and $\alpha^{(2)}$ is the nonlinear polarizability of the molecules in esu. If we choose the reasonable values of $N_A \sim 4 \times 10^{14}$ /cm^2, $\alpha^{(2)} \sim 10^{-30}$ esu, $\mathcal{P}_1 T/A \sim 20$ mJ/cm^2 at $\lambda = 1.06$ μm, $A \sim 0.2$ cm^2, and $T \sim 10$ nsec, we find $S \sim 60$ photons/pulse, which as a highly directional coherent output, is readily detectable. With the pulse energy limited to below the damage threshold, the signal can be further enhanced by orders of magnitude using picosecond pulses and/or surface plasmon pump fields. In addition, $\alpha^{(2)}$ for molecules adsorbed on surfaces may be larger than 10^{-30} esu as a result of molecular alignment and molecule-surface interaction.

Experimentally, second harmonic reflection from a surface of metal or semiconductor with inversion symmetry can be easily detected using a simple setup as shown in Fig. 4. In those cases, the pump beam only penetrates few hundred

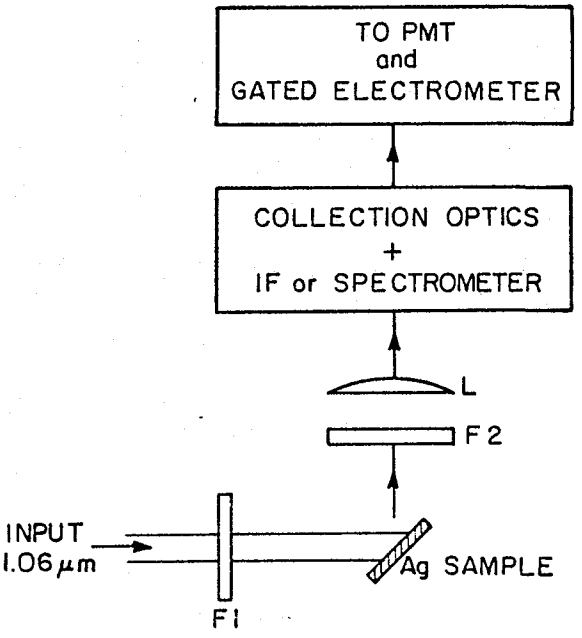

Fig. 4. Experimental setup for second harmonic reflection measurements.

Å into the sample. The second harmonic signal is believed to come mainly from the first one or two surface atomic layers [12]. Submonolayer coverage of sodium on germanium can be detected by an increase in the second harmonic reflection [21]. More recently, we have been able to detect a monolayer of p-nitrobenzoic acid on sapphire or aluminum oxide and rhodamine 6G on glass [22]. To demonstrate the possibility of doing monolayer spectroscopy with a second-order nonlinear optical process, we have also measured the second harmonic output as a function of the pump frequency. Indeed, a resonant peak is observed when 2ω is scanned through the $S_0 - S_2$ transition of the Rhodamine 110 monolayer [22].

As a natural extension, one would use sum-frequency generation for spectroscopic studies of molecular monolayers. The signal strength is expected to be roughly the same as that of second harmonic generation. If one of the beams is

tunable in the infrared, then the frequency dependence of the sum-frequency output yields the vibrational spectrum of the adsorbed molecules.

SURFACE ENHANCED NONLINEAR OPTICAL EFFECTS

We have seen that the field intensity at a smooth metal-dielectric interface can be greatly enhanced through excitation of surface plasmon waves. The same should be true on a rough metal surface. In the latter case, the surface plasmon can be excited directly by shining the beam on the surface because the rough structure can be regarded as a set of random gratings and the surface plasmon can be excited through the grating coupling. On a very rough metal surface, localized surface plasmons can exist on local surface structure of dimension much smaller than a wavelength and enhance the local field around the structure. To illustrate this, consider a metal sphere immersed in a dielectric medium with radius much smaller than a wavelength. Then, in the presence of an incoming beam, the optical field distribution around the sphere can be calculated using the electrostatic approximation [23]. The solution of the problem is well known [24]. The field at a distance $r \geqslant a$ from the center of the sphere is given by

$$\vec{E}_{\ell oc}(\vec{r}) = \overleftrightarrow{L}(\vec{r}) \cdot \vec{E}$$

$$\overleftrightarrow{L}(\vec{r}) = \left(\frac{\varepsilon_M - \varepsilon_D}{\varepsilon_M + 2\varepsilon_D}\right)\left(\frac{a}{r}\right)^3 \overleftrightarrow{K} + 1 \qquad (9)$$

where E is the incoming field and $\overleftrightarrow{K}$ is a constant. The quantity L here plays the role of a local field correction factor. It is seen that $L \propto (\varepsilon_M + 2\varepsilon_D)^{-1}$ which is strongly enhanced if $\mathrm{Re}(\varepsilon_M + 2\varepsilon_D) = 0$. Vanishing of $\mathrm{Re}(\varepsilon_M + 2\varepsilon_D)$ is possible with $\varepsilon_M < 0$ and represents the local surface plasmon resonance of the metal sphere. Equation (9) shows that at this resonance the local field is greatly enhanced and proportional to $\mathrm{Im}(\varepsilon_M + 2\varepsilon_D)$. Also, the field, having an r^{-3} dependence, drops off rapidly with increasing r. Therefore, the optical response from the medium may be strongly dominated by the immediate region around the resonant local structure. This is particularly true for nonlinear optical effects.

More generally, the local field correction factor for a local metal structure of general shape is expected to have a form $L \propto [f(\varepsilon_M/\varepsilon_D)]^{-1}$. The local surface plasmon resonance occurs when Ref = 0. The local field is also expected from the well-known lightning rod effect to be stronger on a more pointing structure [25]. Because of the big local field enhancement due to local surface plasmon resonance, surface nonlinear optical effects at a very rough metal-dielectric interface can be greatly enhanced. Since the nonlinearly induced dipole is now given by $p^{(n)}(\omega) = \alpha^{(n)} E_{\ell oc}(\omega_1)$ --- $E_{\ell oc}(\omega_n)$ instead of $p^{(n)}(\omega) = \alpha^{(n)} E(\omega_1)$ --- $E(\omega_n)$ which is true in the absence of the local metal structure, the output, being proportional to $L^2(\omega)\left|p^{(n)}(\omega)\right|^2$, is enhanced by a factor

$$\eta_\ell = L^2(\omega) L^2(\omega_1) \text{ --- } L^2(\omega_n). \qquad (10)$$

This has not taken into account possible further enhancement from increase of $\alpha^{(n)}$ due to molecule-metal interaction at the interface. The latter certainly contributes to the recently discovered surface enhancement on Raman scattering [26], but is not generally believed to be the dominant mechanism for the observed enhancement.

Now, on a surface with random rough structure, $L(\omega)$ varies over the surface. Different local structures are resonant at different frequencies, and therefore the same local structure cannot be expected to yield maximum local field correction at two very different frequencies. The observed enhancement η should be an average over the surface

$$\eta = \frac{1}{A}\int dA\eta_\ell$$
$$\sim (\eta_\ell)_{max} f$$

where f is the fraction of the surface area with maximum enhancement. The above argument leads to the following predicted enhancement for the various nonlinear optical effects. For second harmonic generation, $\eta(2\omega) \sim [L^4(\omega)L^2(2\omega)]_{max} f \sim L^4_{max}(\omega) f$. For sum-frequency generation, $\eta(\omega_1 + \omega_2) \sim [L^2(\omega_1)L^2(\omega_2)L^2(\omega)]_{max} f \sim L^2_{max}(\omega_1) f$ if the local structure is resonant at ω_1. For third harmonic generation, $\eta(3\omega) \sim [L^6(\omega)L^2(3\omega)]_{max} f \sim L^6_{max}(\omega) f$. For Raman scattering, since the scattering cross-section σ is proportional to $\alpha^{(3)}(\omega_s = \omega_\ell - \omega_\ell + \omega_s)$, the enhancement is $\eta_R \sim [L^2(\omega_\ell)L^2(\omega_s)]_{max} f \sim L^4_{max}(\omega_\ell) f$ if the Raman shift is small so that $\omega_\ell \sim \omega_s$. For CARS output at $\omega_a = 2\omega_\ell - \omega_s$, the enhancement is $\eta(\omega_a) \sim [L^4(\omega_\ell)L^2(\omega_s)L^2(\omega_a)]_{max} f \sim L^8_{max}(\omega_\ell) f$ if the Raman shift is small. As an example, if we choose $L_{max}(\omega) \sim 20$ and $f = 0.05$ for a rough silver surface, we find for second harmonic generation and Raman scattering, $\eta \sim 10^4$; for sum-frequency generation, $\eta \sim 20$; for third harmonic generation, $\eta \sim 3 \times 10^6$; and for CARS, $\eta \sim 10^9$. Such large enhancement should, of course, be readily observable. The big increase in the signal from the immediate neighborhood of the rough metal structure greatly facilitates the surface monolayer detection.

The recent discovery of surface enhanced Raman scattering has attracted a great deal of attention [26]. An enhancement of $\sim 10^6$ in Raman intensity per molecule is observed for molecules on a rough silver surface. While enhancement up to $\sim 10^2$ may come from molecule-silver interaction, the rest is believed to be due to the local field enhancement originated from surface plasmon resonance. The large overall enhancement makes the Raman spectroscopic measurement on adsorbed submonolayer of molecules a fairly simple matter.

Surface enhancement of second harmonic generation has also been observed [9]. In this case, since a smooth bare metal surface can already yield a detectable signal, and no adsorbed molecule on the surface is needed for the measurement, the enhancement can be obtained directly by comparing the second harmonic signals from a smooth surface and a rough surface, and is solely due to the local field increase. The experimental results obtained by Q-switched Nd:YAG laser pulses on silver using the setup of Fig. 4 are given in Fig. 5. The second harmonic signal at 5320 Å shows a quadratic dependence on the input laser power. The signal from the electrolytically roughened surface is 10^4 times larger than that from the smooth evaporated surface. Surface enhanced second harmonic generation has also been observed on copper and gold. The enhancement is only $\sim 10^3$. This can be understood from the smaller value of $L(\omega)$ owing to the larger values of Imε for copper and gold.

Other surface enhanced nonlinear optical effects have also been observed. For example, the sum-frequency generation from a rough silver surface with $\lambda_1 = 1.06$ μm and $\lambda_2 = 0.53$ μm shows an enhancement of ~ 10 as predicted [22]. Among others, surface enhancement of one-photon [27] and multiphoton [9] excited luminescence, hyper Raman scattering [28], third harmonic generation [29], and four-wave mixing [29] have also been seen. In most cases, the actual enhancement factor is difficult to measure because the signal from a smooth surface is far from being detectable as one would predict from estimates. The mere fact that these processes can be observed on a rough surface indicates an extremely large surface enhancement.

DETECTION OF ADSORBED MOLECULES BY SECOND HARMONIC GENERATION ON A SILVER ELECTRODE

The very large surface enhancement should permit an easy detection of ad-

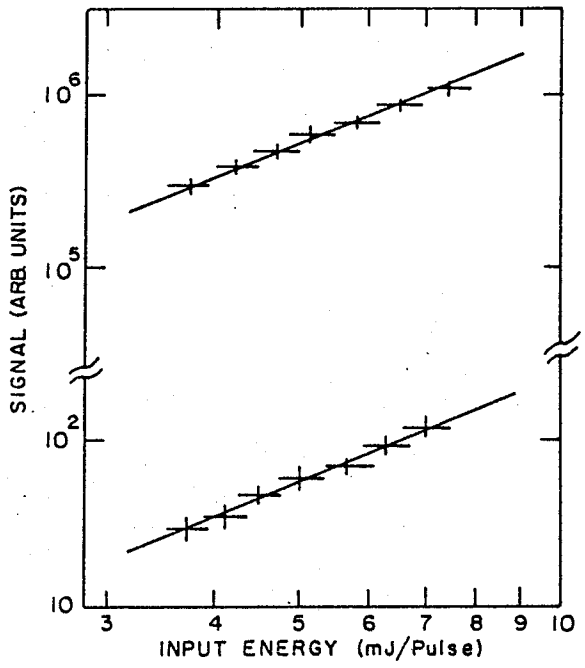

Fig. 5. Power-law dependences of the nonlinear signal on silver. The upper and lower solid curves show the quadratic dependence of the diffuse SH signal from the rough bulk sample and of the collimated SH signal from the smooth film, respectively.

sorbed molecular monolayers on the rough metal surfaces as long as the nonlinear susceptibility of the adsorbed molecules is larger than that of the metal [10]. This is easily demonstrated by monitoring the second harmonic signal from the silver electrode submerged in the electrolytic cell (see Fig. 6) dur-

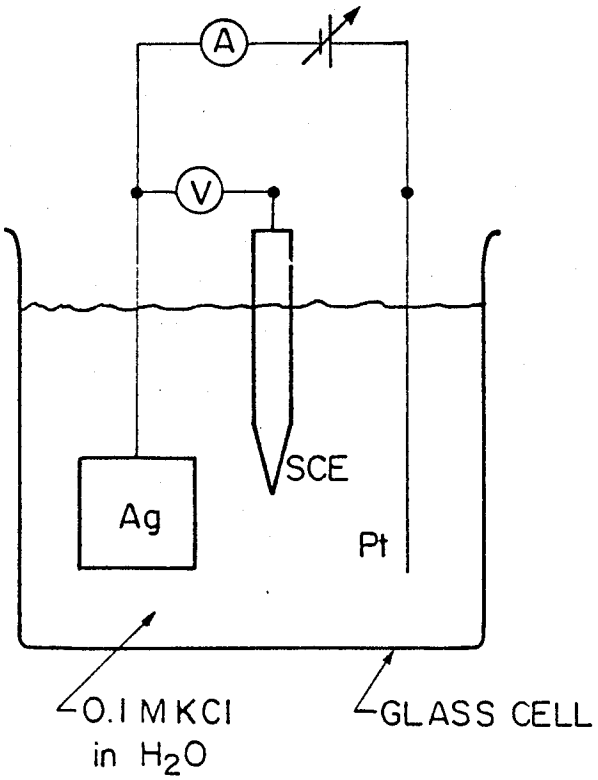

Fig. 6. Electrolytic cell for measurements of surface enhanced optical effects.

ing the oxidation-reduction cycle. The silver surface is first roughened by one or two electrolytic cycles. The second harmonic signal from the roughened surface is then monitored in a subsequent cycle. The result of a typical run is shown in Fig. 7. At the beginning of the oxidation cycle, the signal rises

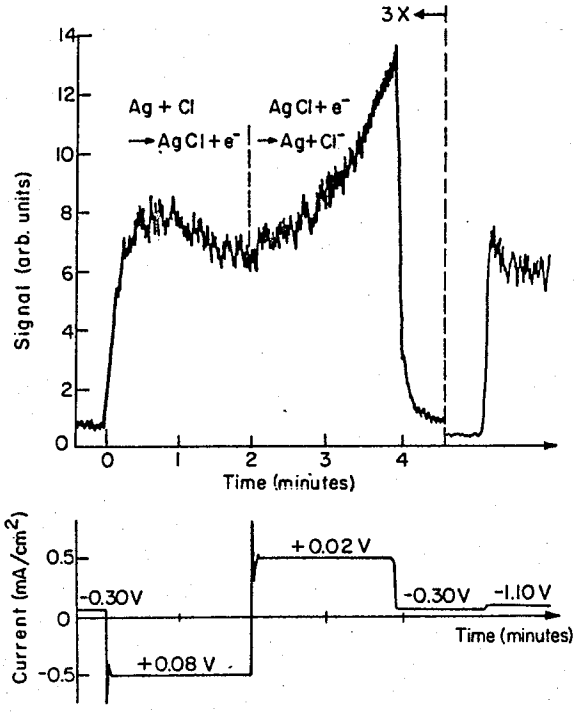

Fig. 7. Current and diffuse SH as a function of time during and after an electrolytic cycle. The voltages listed in the lower curve are V_{Ag-SCE}. Pyridine (.05M) was added to the 0.1M KCℓ solution following the completion of the electrolytic cycle.

sharply as AgCℓ is formed on the electrode. It soon levels off after the formation of 3 or 4 monolayers of AgCℓ on average, judging from the amount of charge transfer that has occurred. This can be explained knowing that only the surface molecular layers should contribute to second harmonic generation. The signal variation during the oxidation-reduction cycle, especially the monotonic increase during the reduction period, is probably due to change of surface roughness through removal and redeposition of silver. Finally, at the end of the reduction cycle, the signal drops suddenly as the last 3 or 4 layers of AgCℓ are reduced. In the present case, field-induced second harmonic generation is not responsible for the observed signal because the latter is insensitive to the bias voltage V_{Ag-SCE} and remains unchanged when the oxidation or reduction process is stopped in the middle of the cycle.

After the oxidation-reduction cycle, if pyridine (0.05M) is added to the electrolytic solution and a negative bias of $V_{Ag-SCE} \sim -1.1$ v is applied, the second harmonic signal increases by 25-50 times (see Fig. 7). From the results of electrochemistry and surface enhanced Raman scattering, it is known that the negative bias causes a monolayer of pyridine molecules to be adsorbed on the silver electrode. Therefore, the signal increase must come from the adsorbed pyridine monolayer. In the experiment, an input pulse of 0.2 mJ at 1.06 μm focused to a 0.2 cm^2 spot on the silver electrode is used. The second harmonic output is as strong as 8×10^5 photons/pulse. The corresponding nonlinear polarizability $\alpha^{(2)}$ for the adsorbed pyridine molecule is found to be 2×10^{-29} esu if the surface enhancement on the rough electrode is assumed to be 10^4. This value of $\alpha^{(2)}$ seems to be larger than one normally expects for similar molecules ($\sim 10^{-30}$ esu) [30]. It is possible that $\alpha^{(2)}$ may have been enhanced through the molecule-metal interaction.

The adsorption of pyridine on silver is known to depend on the bias voltage V_{Ag-SCE}. The second harmonic signal from pyridine is a crude measure of the amount of pyridine adsorbed on silver. The data in Fig. 8 show that pyridine begins to be adsorbed at $V_{Ag-SCE} \sim -0.6$ v and reaches a monolayer at ~ -0.9 v.

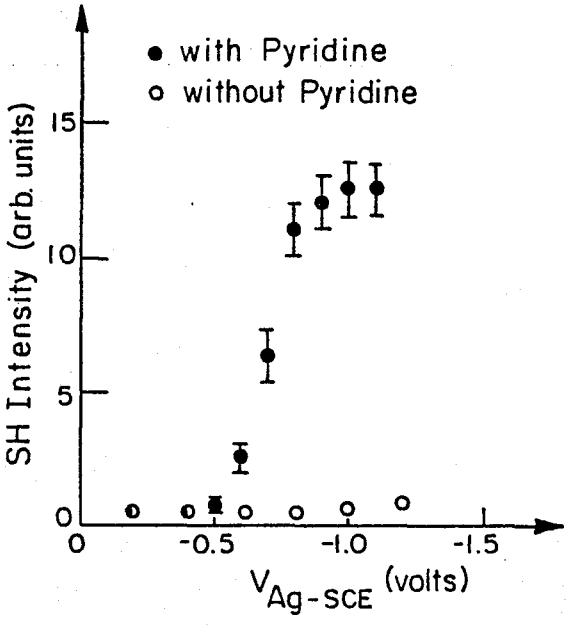

Fig. 8 Diffuse second harmonic signal versus V_{Ag-SCE} following an electrolytic cycle, with .05M pyridine and 0.1M KCℓ dissolved in water.

We can in fact use second harmonic generation to obtain an adsorption isotherm, i.e., the surface density of adsorbed pyridine molecules versus pyridine concentration in the electrolytic solution [31]. The second harmonic signal can be written as $\mathcal{P}(2\omega) = (A + BN_A)^2$, where A is from silver and BN_A from the adsorbed pyridine with N_A being its surface density. Figure 9 shows the exper-

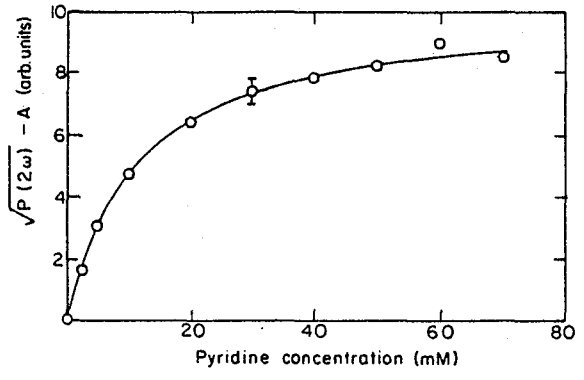

Fig. 9. Equilibrium ($\sqrt{P(2\omega)}$ - A) versus bulk pyridine concentration. The solid curve is a theoretical fit to the expermental data using the Langmuir model.

imental result of $[\sqrt{\mathcal{P}(2\omega)} - A] \propto N_A$ versus the pyridine concentration ρ for $V_{Ag-SCE} = -1.0$ v in a 0.1M KCℓ aqueous solution. As shown, the data can be fit very well by the simple Langmuir equation [32]

$$N_A = \frac{\rho}{K + \rho} N_{AS} \tag{11}$$

where N_{AS} is the saturated value of N_A and K (in mole/ℓ) is related to the adsorption free energy ΔG by

$$K = 55 \exp(-\Delta G/RT).$$

The theoretical fit in Fig. 9 yields a value of ΔG = 5.1 KCal/mole for pyridine on silver. A similar adsorption isotherm can also be obtained by surface enhanced Raman scattering; the initial slope of the curve is somewhat higher, yielding a somewhat higher adsorption free energy ΔG = 5.7 KCal/mole.

Surface enhanced second harmonic generation from other molecules adsorbed on silver, such as CN, pyrazine, etc., can also be detected. It is interesting to compare the results of pyridine and pyrazine. The pyrazine molecule  is centrosymmetric, but the pyrazine molecule  is not. Therefore, for isolated molecules, $\alpha^{(2)} = 0$ for pyrazine and $\alpha^{(2)} \neq 0$ for pyridine. If the molecules are adsorbed on a surface, however, both can have nonvanishing $\alpha^{(2)}$ because the molecule-surface interaction breaks the symmetry. How much $\alpha^{(2)}$ is changed, of course, depends on how strong the molecule-surface interaction is. The second harmonic signal from pyrazine versus V_{Ag-SCE} is shown in Fig. 10 [33]. Its maximum is about 4 times smaller than that from pyridine, indicating

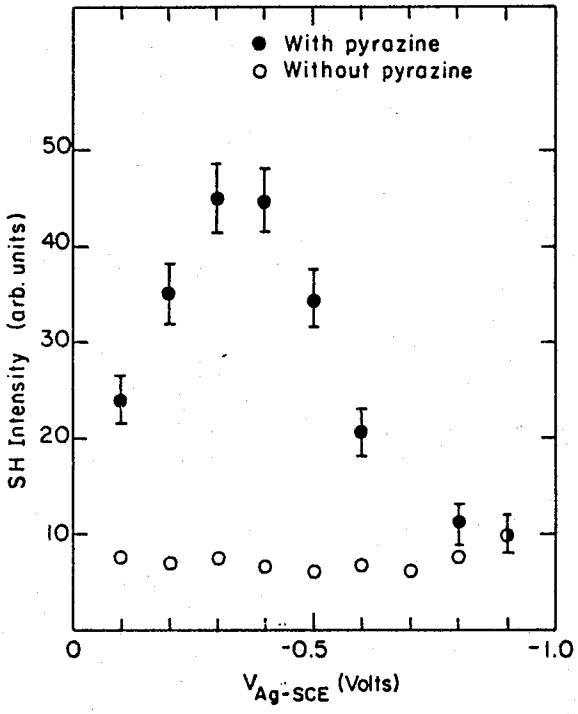

Fig. 10. Diffuse second harmonic signal versus V_{Ag-SCE} following an electrolytic cycle in 0.1M KCl, with and without .05M pyrazine present.

that $\alpha^{(2)}$ for pyrazine is only 2 times less than $\alpha^{(2)}$ for pyridine. This leads to the conclusion that pyrazine is chemically adsorbed on silver with a fairly strong pyrazine-silver interaction. The same conclusion has been obtained from Raman measurements.

In principle, since second harmonic generation from a smooth metal surface can be detected, that from an adsorbed molecular monolayer should also be detectable as long as the second-order nonlinearity of the molecules is larger than that of the metal. Then, surface enhancement is not needed for monolayer detection. In practice, monolayer adsorption of molecules on a smooth metal surface can often be prepared only in ultrahigh vacuum systems.

DISCUSSION

In this section, we consider the advantages and disadvantages or possible difficulties of the various nonlinear optical techniques for surface studies. The common advantages of all nonlinear optical techniques as compared to the existing techniques are their capabilities for in-situ measurements under different environmental conditions, high-resolution spectroscopic studies, and

transient studies with picosecond resolution. The disadvantages usually arise from the presence of an unwanted background signal and the requirement of an appropriate laser system with a broad range of tunability. Surface damage and desorption of molecules by laser heating limit the input laser power. This may also lead to difficulty.

Specifically, the various techniques have their own strong and weak points. Surface enhanced Raman scattering has high sensitivity and good spectral resolution over the entire vibrational spectroscopic range. It would be an ideal tool for surface studies, but unfortunately, the surface enhancement effect is appreciable only on very few metals, and the rough surface condition makes the analysis of results extremely difficult. Other surface enhanced nonlinear optical processes have similar difficulties.

Second harmonic generation can be more sensitive than Raman scattering, and presumably can be used to study not only gas-solid interface but also liquid-solid interface. However, the process with a fixed pump laser frequency is not spectrally selective (it resembles ellipsometry in this respect), and it is often difficult to discriminate the signal from the adsorbed molecules from that of the substrate, especially if the latter is larger than or comparable to the former. On a rough surface, the second harmonic output is diffuse in all directions. Then, the luminescence background from the substrate, if very strong, may also become a nuisance. Second harmonic generation with a tunable visible laser allows allows surface spectroscopic studies involving electronic transitions. For studies of vibrational transitions, tunable infrared lasers are needed. Then, for better detection sensitivity, sum-frequency generation with a tunable infrared beam and a visible beam should be used. The technique could have high-resolution and high-sensitivity capability, but unfortunately, high-intensity infrared lasers with tunability over the entire infrared range are not yet available.

Second-harmonic or sum-frequency generation depends to some extent on the molecular orientation on the surface. Thus, measurements with different polarizations may be able to yield information about the orientation of the adsorbed molecules. The polarization dependence may also be used to suppress the background signal from the substrate.

The Raman gain spectroscopy also has high sensitivity and spectral resolution, and is capable of suppressing the luminescence and nonresonant background. It, however, requires two stable synchronously pumped CW picosecond dye lasers. The thermal effect caused by laser heating of the substrate yields, on the other hand, a background signal that limits the detection sensitivity. At present, the Raman gain measurement on a molecular monolayer is still a very difficult task.

Coherent antiStokes Raman scattering with surface plasmons may prove to be extremely sensitive with picosecond pulses. Like other Raman spectroscopy, it easily covers the entire vibrational spectroscopic range. Its sensitivity will, however, be limited by the nonresonant background coming from the four-wave mixing process in the metal or substrate. Polarization dependence can perhaps be used to suppress the background. The requirement of surface plasmon excitation makes the experimental arrangement somewhat difficult.

In conclusion, we should point out that the development of nonlinear optical techniques for surface studies has only begun very recently. Many difficulties are yet to be overcome. The initial results have, however, suggested a rather bright future for these techniques. It is anticipated that in another few years they could become a new class of useful tools for studies of both surface statics and surface dynamics.

ACKNOWLEDGMENTS

The author acknowledges valuable discussions with C. K. Chen, A. R. B. de

Castro, T. F. Heinz, and D. Ricard, who have carried out the experimental work on surface nonlinear optics in our laboratory. This work was supported by the Director, Office of Energy Research, Office of Basic Energy Sciences, Materials Sciences Division of the U. S. Department of Energy under Contract No. W-7405-ENG-48. YRS also acknowledges a research professorship from the Miller Institute of the University of California.

REFERENCES

1. See, for example, G. Somorjai, Chemistry in Two Dimensions (Cornell University Press, Ithaca, NY, 1981).

2. P. K. Hansma, Phys. Rev. 30C, 145 (1977).

3. J. Pritchard and T. Catterick, in Experimental Methods in Catalytic Research, Vol. III, ed. by R. B. Anderson and P. T. Dawson (Academic Press, NY, 1976).

4. R. B. Bailey, T. Iri, and P. L. Richards, Surface Science 100, 626 (1980).

5. C. K. Chen, A. R. B. de Castro, Y. R. Shen, and F. DeMartini, Phys. Rev. Lett. 43, 946 (1979).

6. J. P. Heritage, in Picosecond Phenomena II, ed. by R. M. Hochstrasser, W. Kaiser, and C. V. Shank (Springer-Verlag, Berlin, 1980), p.343; J. P. Heritage and D. L. Allara, Chem. Phys. Lett. 74, 507 (1980).

7. B. F. Levine, C. G. Bethea, A. R. Tretola, and M. Korngor, Appl. Phys. Lett. 37, 595 (1980).

8. M. Fleischmann, P. J. Hendra, and A. J. McQuillan, Chem. Phys. Lett. 26, 163 (1974); D. L. Jeanmaire and R. P. Van Duyne, J. Electroanal. Chem. 84, 1 (1977).

9. C. K. Chen, A. R. B. de Castro, and Y. R. Shen, Phys. Rev. Lett. 46, 145 (1981).

10. C. K. Chen, T. F. Heinz, D. Ricard, and Y. R. Shen, Phys. Rev. Lett. 46, 1010 (1981).

11. Y. R. Shen and F. DeMartini, in Surface Polaritons, ed. by V. M. Agranovitch and D. L. Mills (North Holland Publishing, Amsterdam, 1981), Chapter 14.

12. N. Bloembergen and P. S. Pershan, Phys. Rev. 128, 606 (1962); N. Bloembergen, R. K. Chang, S. S. Jha, and C. H. Lee, Phys. Rev. 174, 813 (1968).

13. J. Song and M. D. Levenson, J. Appl. Phys. 48, 3496 (1977).

14. A. Sommerfeld, Ann. Physik 28, 665 (1909).

15. H. J. Simon, R. E. Benner, and J. G. Rako, Optics Comm. 23, 245 (1977).

16. E. Kretschmann, Z. Phys. 241, 313 (1971).

17. F. DeMartini and Y. R. Shen, Phys. Rev. Lett. 36, 216 (1976).

18. C. K. Chen, A. R. B. de Castro, and Y. R. Shen (unpublished).

19. A. Owyoung, IEEE J. Quantum Electron. QE-14, 192 (1978).

20. J. P. Heritage, Appl. Phys. Lett. 34, 470 (1979); B. F. Levine, C. V. Shank, and J. P. Heritage, IEEE J. Quantum Electron. QE-15, 1418 (1979).

21. J. M. Chen, J. R. Bower, C. S. Wang, and C. H. Lee, Optics Comm. 9, 132 (1973).

22. T. F. Heinz, C. K. Chen, D. Ricard, and Y. R. Shen (unpublished).

23. S. M. McCall, P. M. Platzman, and P. A. Wolff, Phys. Lett. 77A, 331 (1980).

24. See, for example, J. D. Jackson, Classical Electrodynamics (John Wiley, New York, 2nd ed., 1975), p.150.

25. J. I. Gersten and A. Nitzan, J. Chem. Phys. 73, 3023 (1980).

26. See, for example, the review article by R. P. Van Duyne, in Chemical and Biological Applications of Lasers, ed. by C. B. Moore (Academic Press, NY, 1978), vol.4.

27. A. M. Glass, P. F. Liao, J. G. Bergman, and D. H. Olson, Optics Lett. 5, 368 (1980).

28. R. K. Chang (private communication).

29. G. T. Boyd, Z. H. Yu, and Y. R. Shen (unpublished).

30. J.-L. Oudar and H. LePerson, Opt. Comm. 15, 258 (1975); J.-L. Oudar and D. S. Chemla, Opt. Comm. 13, 164 (1975).

31. C. K. Chen, T. F. Heinz, D. Ricard, and Y. R. Shen, Chem. Phys. Lett. (to be published).

32. See, for example, M. J. Rosen, Surfectants and Interfacial Phenomena (John Wiley, New York, 1978), Chapter 2.

33. T. F. Heinz, C. K. Chen, D. Richard, and Y. R. Shen, Chem. Phys. Lett. (to be published).